



e-ISSN: 2319-8753 | p-ISSN: 2347-6710

IJRSET

International Journal of Innovative Research in
SCIENCE | ENGINEERING | TECHNOLOGY



INTERNATIONAL JOURNAL OF INNOVATIVE RESEARCH

IN SCIENCE | ENGINEERING | TECHNOLOGY

Volume 13, Issue 4, April 2024

ISSN INTERNATIONAL
STANDARD
SERIAL
NUMBER
INDIA

Impact Factor: 8.423

9940 572 462

6381 907 438

ijrset@gmail.com

www.ijrset.com

Reducing Soft-Switching Losses Of IGBTs By Dual-Active-Bridge Dc/Dc Converters

P.Praveen¹, Deepika², R.Manish³, K.Soujanya⁴

UG Student Department of Electrical and Electronics Engineering, CMR College of Engineering & Technology, Hyderabad, Telangana, India^{1,2,3}

Professor, Department of Electrical and Electronics Engineering, CMR College of Engineering & Technology, Hyderabad, Telangana, India⁴

ABSTRACT: Soft-switching methods are not only highly desired but often essential needs in medium-voltage and medium-frequency applications such as solid-state transformers. The successful use of these soft-switching techniques is directly attributed to the dynamic behavior of the internal stored charge in the semiconductor devices that are utilized. For this reason, this project analyzes the behavior of the internal charge dynamics in high-voltage (HV) semiconductors. This offers a strong basis for understanding the zero current-switching methods previously presented for insulated-gate bipolar transistor (IGBT)-based resonant dual active bridges, as well as for executing overall converter optimizations. One of the main concepts that have been found to be involved in lowering switching loss in HV semiconductors by tailoring the conducted current to obtain a high recombination time in the previously conducting semiconductors. A 1.7-kV IGBT-based neutral-point-clamped (NPC) bridge is used to study and validate the benefits of the suggested techniques in MATLAB, as well as how to use them in a triangular-current-mode dual active-bridge converter. The studies were carried out on this particular bridge. The simulation results are used to demonstrate the recommended approach, which is used to improve output using MATLAB Simulink.

KEYWORDS: Tailoring, Striving, Lacking

I. INTRODUCTION

Today's electric power networks rely heavily on TRANSFORMERS running at line frequency (50 Hz/60 Hz), which act as a connection between grids with varying voltage levels, such as high-voltage (HV), medium-voltage (MV), and low-voltage (LV) grids. However, these transformers have a number of drawbacks, including their considerable size and weight, their ideally equal active and reactive power levels, their equally connected input and output voltages, and their equal input and output working frequencies. By creating a solid-state transformer (SST), a transformer based on power electronics, these restrictions can be removed. Fig1 illustrates a single-phase SST in action. The MV side ac/ac converter is used to actively shape the input current i_{MV}^{MV} , for example, to reach a unity power factor or in other cases, to act as an active filter and/or a static var compensator.

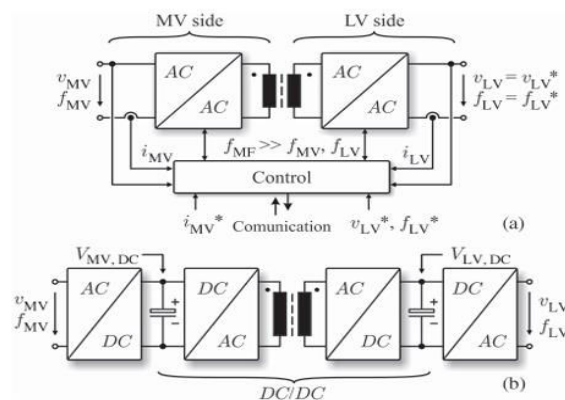


fig 1:(a)single phase structure (b)three phase structure of ac/ac converter

The MV side ac/ac converter is used to actively shape the input current i^{MV} , for example, to reach a unity power factor or in other cases, to act as an active filter and/or a static var compensator. The link between the MV and the LV ac/ac converters is done through a transformer whose operating frequency f^{MF} lies in the medium-frequency (MF) range, thus achieving a small size/weight and a faster dynamic response. On the LV side, the characteristics of the output ac voltage, namely, amplitude V_{LV} and frequency f_{LV} , can be actively controlled with little dependence on the MV side voltage V_{MV} and frequency f_{MV} . These additional functionalities are envisioned as the key enabling features for future compact traction solutions grid integration of renewable energy generation, and smart grid implementation among others.

One possible structure for the SST is a three-stage concept presented in Fig1(b). In this concept, ac/dc MV and LV converters are connected to the MV and LV ac grids, respectively. The dc links of these ac/dc converters are linked through a high-power dc/dc converter, where the isolation and voltage step-down is provided through an MF ac link. In the dc/dc converter, the semiconductors in the MV side bridge are required to block voltages in the kilovolt range; therefore, IGBTs are a very attractive choice. These semiconductors, however, are characterized by a bipolar power stage that, in order to block these HVs, comprises a considerably large N-base region, which stores a large amount of charge during the conduction phase of the semiconductor. When the switch is turned off, this stored charge is evacuated from the semiconductor, causing tail currents that overlap with the blocking voltage, hence generating high switching losses. If operated in the MF range, these switching losses would be unbearable, unless the current through the semiconductors is conveniently shaped during its conduction phase in order to achieve zero-current switching (ZCS). A widespread topology that can allow bidirectional power flow and ZCS operation, investigated mainly in traction applications, is the half-cycle discontinuous-conduction-mode series resonant converter (HC-DCM-SRC). This topology consists of two active bridges linked through an MF transformer in series with a resonant tank. The MV and LV side switches can function in ZCS, which lowers their switching losses, when this converter is run below resonance frequency.

Nevertheless, these switching losses are not negligible despite ZCS operation. For this reason, several enhancements to the ZCS modulation scheme that allow a further reduction in the switching losses. The main disadvantage of the HC-DCM-SRC, in addition to its lower power density and high current requirement of the series resonant capacitor C_r , is its incapability to control the transferred power while still achieving ZCS. The triangular-current-mode dual active bridge (TCM DAB) is a desirable option if power transfer management is needed. A series inductor L_s is used in this converter in place of the resonant tank. The MV side switches may be operated in ZCS mode in both power directions by appropriately choosing the transformer turns ratio, and the transferred power can be actively controlled by varying the LV side duty cycle. In this case, however, it is not possible to achieve ZCS on the LV side. The crucial component of the converter modeling that is lacking in order to enable an overall system optimization—such as striving for maximum power density or efficiency—is an accurate model for calculating the switching losses in these ZCS-operated converters. Prior research has been published in the literature on the dynamics of internal charge behavior in IGBTs. Nevertheless, in order to carry out the previously indicated overall system optimization, a straightforward model that connects the conducted current of the semiconductors to the dynamics of stored charge has not been examined in these works.

II. MOTIVATION

The primary goal for this project is to minimize switching losses in semiconductor devices. During the semiconductor's conduction phase, these semiconductors store a significant quantity of charge. This stored charge is released from the semiconductor when the switch is switched off, creating tail currents that overlap with the blocking voltage and leading to significant switching losses. These switching losses would be intolerable if the semiconductors were operated in the MF range, unless zero-current switching (ZCS) could be achieved by easily shaping the semiconductors' current during its conduction phase. By using TCM-DAB the circuit is enhanced and reduced the loss by using ZCS technics.

III. LITERATURE SURVEY

Bellamkonda Dwiza, Student Member, IEEE discusses the Efficiency Improvement and High-performance Control of Dual-active-bridge (DAB) DC-DC Converter with Triple-phase-shift (TPS) Modulation. The study aims to analyze the optimal switching modes of the DAB DC-DC converter to reduce loss and improve efficiency. The TPS modulation is proposed to decrease reactive power and achieve global optimization of conduction loss and soft-switching. Additionally, a high-dynamic control strategy based on direct-power feed-forward is designed to improve the system's

response to external disturbances. The study introduces the DAB DC-DC converter and its application in high-performance isolated bidirectional DC-DC conversions for electric vehicles and energy stations. Advantages of the DAB converter, such as high power density and environmental adaptability. The study analyzes the switching characteristics of mode 1 and mode 2 under different voltage ratios and discusses the impact of TPS modulation on reducing switching loss and expanding the soft-switching range. The document addresses the issue of dc-offset current in the AC link and proposes methods for its suppression, including both static and dynamic suppression techniques. Finally, the study highlights a high-dynamic control strategy based on direct-power feed-forward to improve the dynamic response to external disturbances.

Shaoduo Zheng and Feng Lyu explores the analysis of common-mode noise and the design of a reduced-volume concentric choke for a dual active bridge (DAB) dc-dc converter with integrated magnetics. The analysis aims to thoroughly understand the common-mode noise performance of the DAB converter employing an integrated transformer. The study highlights the impact of integrating the transformer on the common-mode noise profile and proposes a concentric choke design that occupies less volume compared to its conventional counterpart. The benefits of integrated magnetics, and the analysis and design guidelines for the proposed concentric choke. Additionally, the study experimentally validates the analyses and designs on a DAB converter prototype. It presents the challenges posed by conventional CM chokes in terms of volume and power density and proposes a concentric CM choke design as a solution. The study also discusses the experimental validation of the proposed concentric CM choke on a DAB converter prototype, confirming its effectiveness in reducing common-mode noise within the desired standard.

Qiang Ren, Fei Xiao, Jilong Liu, Peng Chen, and Zhichao Zhu discusses a new approach to designing a compact medium voltage (MV) DC/DC converter using series-connected power devices as switching modules. The proposed converter aims to address the challenges faced by traditional approaches, such as the complexity and high number of components in modular converters and the limitations of new semiconductor power devices. The letter proposes a phase-shifted full-bridge (PSFB) MV DC/DC converter that uses series-connected power devices, requiring only one external isolated driver circuit and a few components for voltage sharing. The operation principle of the switching modules is analyzed, and the feasibility of the design is validated through simulations and experiments. The proposed converter offers advantages in volume, efficiency, reliability, and cost compared to other MV DC/DC converter schemes.

Kambhampati Venkata Govardhan Rao have explored "Design of a bidirectional DC/DC converter for a hybrid electric drive system with dual-battery storing energy" The BDCC facilitates energy flow between dual low-voltage sources and a high-voltage dc bus, allowing bidirectional power flow and efficient energy management. The proposed converter topology and its various operation modes, including twin-source low-voltage powering, energy-regenerating high-voltage dc-link mode, and low-voltage dual-source buck/boost mode, are thoroughly explained. The simulation results demonstrate the performance and viability of the proposed BDCC, showcasing its capability to efficiently manage power flow and meet the requirements of electric and hybrid vehicle systems.

Lan Ma , Hongbing Xu, Alex Q. Huang conducted a comparative analysis on a novel called "IGBT Dynamic Loss Reduction through Device Level Soft Switching" by Lan Ma et al. presents a novel series hybrid switching method to reduce dynamic switching loss in Silicon Insulated Gate Bipolar Transistor (Si IGBT). The paper addresses the challenges associated with Si IGBT's switching losses and proposes a new method to achieve soft switching in both turn-on and turn-off periods. By combining SiC MOSFET and Si IGBT, the proposed method achieves significant reductions in turn-on loss (90%) and turn-off loss (57%). The study also introduces a new soft switching classification considering voltage and current transient states and proposes an improved modulation method to further optimize the performance of the hybrid switches. The introduction establishes Si IGBT's significance in high-power applications and highlights the necessity to minimize switching losses for enhanced efficiency and performance

Klayani Thalanki ,K V goverdhan Rao explored the MATLAB modelling simulation on "Improved Bidirectional dc/dc Converter with Split Battery Configuration for Electric Vehicle Battery Charging/Discharging." The bidirectional converter aims to provide a solution for vehicle-to-grid (V2G) and grid-to-vehicle (G2V) power flow compatibility. It utilizes an isolated configuration to handle high power density at a wide load range, beneficial for electric vehicle (EV) applications. The converter performs step-up and step-down operations with zero voltage switching for all power switches in both directions. During charging, the split of batteries is achieved to facilitate high charging current, and the commutation of switches is achieved at zero voltage switching without snubber circuitry. The proposed topology is simulated using MATLAB/Simulink for a 350W battery system. The document emphasizes the environmental and



economic benefits of electric vehicles (EVs) and hybrid electric vehicles (HEVs) as a solution to the issues of environmental pollution and global warming. The simulation results demonstrate the converter's effectiveness in achieving low losses, natural voltage clamping, and soft switching, which contribute to improved voltage regulation and better performance during charging and discharging modes. Overall, the study presents a comprehensive exploration of the improved bidirectional dc/dc converter with split battery configuration for EV battery charging/discharging. The proposed converter offers several advantages, including high power density, reduced losses, and improved battery charging efficiency. The simulation results validate the theoretical concepts and demonstrate the converter's ability to facilitate efficient charging and discharging of electric vehicle batteries, thereby contributing to the advancement of electric vehicle technology.

IV. SEMICONDUCTOR STORED CHARGE DYNAMICS

HV bipolar semiconductor devices, as aforementioned, store large amounts of charge during their conduction phases. This charge, if not allowed to recombine internally, is translated into switching losses when the device is taken back to the blocking state. Since this stored charge is directly related to the dissipated energy during the switching process, it is useful to analyze the behavior of the charge $Q(t)$ stored in the switch during its conduction phase. The minority carrier (hole) concentration $p_0(t)$ in the N-base layer must first be examined in order to carry out this investigation. Examine the following expression to understand the relationship between the hole current density (diffusion current) $J_{p0}(t)$ and the carrier concentration $p_0(t)$:

$$p_0(t) = \frac{L_a}{2qD_p} \tanh\left(\frac{W_N}{L_a}\right) J_{p0}(t) \quad (1)$$

$$L_a = \sqrt{\tau D_a} \quad (2)$$

Where L_a is the ambipolar diffusion length, D_p is the hole diffusion constant in the N-base layer, W_N is the thickness of the N-base layer, q is the electron charge, τ is the recombination time constant, and D_a is the ambipolar diffusion constant. Within the N-base layer, the carrier distribution decays exponentially due to recombination hence

$$p(x, t) = p_0(t) \cdot e^{-\frac{x}{L_a}}$$

Integrating over the N base layer and multiplying by the elementary electric charge q and the device area S gives the total charge $Q(t)$ in the N-base layer.

$$Q(t) = qS \int_0^{W_N} p(x, t) \cdot dx \quad (4)$$

$$= qS \cdot L_a \cdot p_0(t) \cdot \left(1 - e^{-\frac{W_N}{L_a}}\right) \quad (5)$$

This charge $Q(t)$ recombines in a loss less manner as long as the collector-emitter voltage V_{CE} remains close to zero. If a positive collector-emitter voltage V_{CE} is applied to the device before total recombination is achieved, the remaining charge will be externally removed from the N-base layer, causing switching losses in the semiconductor. In HV devices, the N-base layer width W_N is made large in order to withstand the blocking voltage. In (5), it is shown that a large N-base directly increases the amount of stored charge $Q(t)$ in the device, hence increasing the switching losses. Additionally, in HV devices, the carrier life time τ is made long in order to decrease the ON-state voltage, which increases the amount of stored charge. In some applications, however, lifetime control can be applied in order to decrease the lifetime τ , i.e., reducing switching losses, but with increased ON-state voltage and hence higher conduction losses. In order to calculate the instantaneous value of stored charge $Q(t)$ for an arbitrary currents $i(t)$, the following equation, the time-dependent bipolar diffusion equation, is used

$$\frac{dp(x, t)}{dt} = -\frac{p(x, t)}{\tau} + D_a \frac{d^2 p(x, t)}{dx^2} \quad (6)$$

Which is valid while the collector–emitter voltage VCE is constant and ≈ 0 V. By differentiating (4) with respect to time and combining with (6), the following expression is obtained:

$$\begin{aligned} \frac{dQ(t)}{dt} &= qS \int_0^{W_N} \left(-\frac{p(x,t)}{\tau} + D_a \frac{d^2 p(x,t)}{dx^2} \right) dx \\ &= -qS \frac{L_a}{\tau} \cdot p_0(t) \cdot \underbrace{\left(1 - e^{-\left(\frac{W_N}{L_a}\right)} \right)}_{\frac{Q(t)}{\tau}} \\ &\quad + qS \frac{D_a}{L_a} p_0(t) \left(1 - e^{-\left(\frac{W_N}{L_a}\right)} \right). \end{aligned} \quad (7)$$

The first term on the right-hand side of (7) is equal to $Q(t)/\tau$. Replacing (1) in (7), the following expression is found:

$$\begin{aligned} \frac{dQ(t)}{dt} &= -\frac{Q(t)}{\tau} \\ &\quad + qS \frac{D_a}{L_a} \frac{L_a}{2qD_p} \tanh\left(\frac{W_N}{L_a}\right) \left(1 - e^{-\left(\frac{W_N}{L_a}\right)} \right) J_{p0}(t). \end{aligned} \quad (8)$$

The hole current density $J_{p0}(t)$ is proportional to the total current density $J_s(t)$ through the switch

$$J_{p0}(t) = J_s(t) \cdot K_{p0} = \frac{K_{p0}}{S} \cdot i_s(t) \quad (9)$$

Where $i_s(t)$ is the instantaneous current through the switch, and K_{p0} is the proportional constant relating the total current density $J_s(t)$ to the diffusion current density $J_{p0}(t)$. This constant depends on the switch technology where by the expressions for the field-stop (FS) and non punch through (NPT) technologies can be found in [1]. Replacing (9) into (8) yields

$$\begin{aligned} \frac{dQ(t)}{dt} &= -\frac{Q(t)}{\tau} \\ &\quad + \underbrace{q \frac{D_a}{L_a} \frac{L_a}{2qD_p} \tanh\left(\frac{W_N}{L_a}\right) \left(1 - e^{-\left(\frac{W_N}{L_a}\right)} \right) K_{p0}}_{k_s} \cdot i_s(t). \end{aligned} \quad (10)$$

The constant (non time dependent) part of these cond term on the right-hand side of (10) is condensed into term k_s (with $0 < k_s$)

$$\frac{dQ(t)}{dt} = -\frac{Q(t)}{\tau} + k_s \cdot i_s(t). \quad (11)$$

The simple expression for the dynamic behavior of the stored charge $Q(t)$ in the semiconductor device, where by only parameters τ and k_s are required in order to describe this behavior. These parameters are usually confidential information from the semiconductor manufactures and therefore cannot be extracted from the device's datasheet.

V. PROPOSED SOLUTION OF TCM DAB

The switching losses in the typical ZCS modulation scheme examined in [1] were initially assessed in order to benchmark the suggested modulation techniques for the TCM DAB. As seen in figure 6, these tests were carried out using the previously stated 1.7-kVFS IGBT module (FF150R17KE4), which was intended for nominal power of 166 kW and 20kHz of switching frequency. The bridge was constructed as a 2-kV NPC-based bridge [with super rapid recovery clamping diodes (DSDI 60)]. Figure 6 depicts this bridge's hardware realization. In the third section, we will employ the nonlinear inductor L_{sat} , which is depicted in Figure 6, to shape the current in order to lower the switching losses in

the MV side switches. The LV side bridge is a 400-V full-bridge construction that is used to provide the required current waveforms, and the transformer turns ratio is $N1/N2 = 3/1$.

The voltages and currents in switches S1, S2, S3, and S4 were measured, respectively, using passive voltage probes and planar current transformers.

A detailed description of the operation of the TCM DAB converter together with the respective analytical formulation can be found in[1]. The turn-off and turn-on processes of complementary switches S1 and S3, respectively, are used here in in order to exemplify the ZCS process and the further enhancements. It should be noted, however, that for a comprehensive switching loss analysis, all switching events were measured and used to calculate the total losses in the NPC bridge.

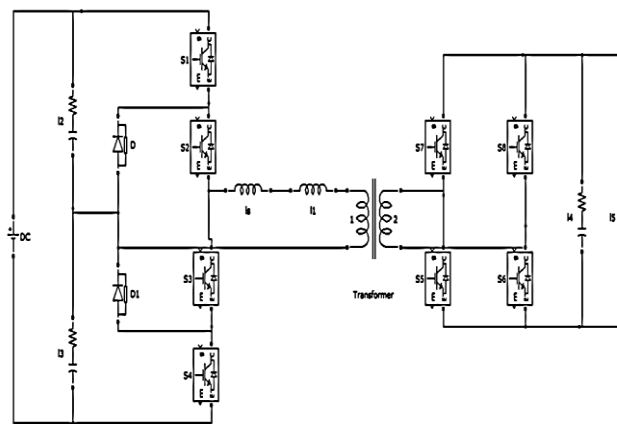


fig:2 DAB converter used to test the 1.7-kV FS IGBTs: (a) NPC-based bridge linked to the LV full bridge through an $N1/N2 = 3/1$ transformer

VI. RESULTS & DRAWINGS

The procedure by which devices S1 and S3 were switched during displays the time interval that is shown in Figure 7, in that order. Since S1 was carrying the current during the positive semicycle, it is evident from this that it contains a significant quantity of charge that is held, which is released when S3 is turned on, resulting in sizeable turn-on losses in S3 and turn-off losses in S1.

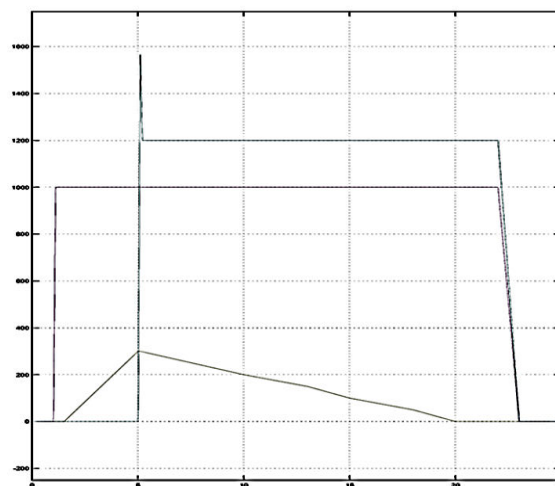


fig:3 Main waveforms in standard ZCS with TCM DAB and power from the MV side to the LV side

The phase shift and duty cycles of the LV and MV side bridges have been changed to produce power flow in the opposite direction while still achieving ZCS on the MV side.

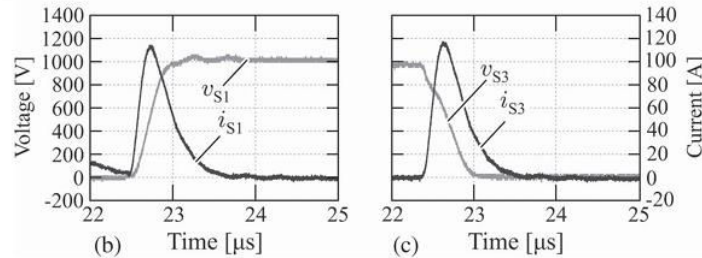


fig:4 ac-link waveforms for half switching period; (b) voltage and current in S1 during the time instant highlighted in (FIG 7); and (c) voltage and current in S3 during the time instant highlighted in (FIG 7).

The current and voltage waveforms in the transformer for power flowing from LV to MV are illustrated in Figures 8 depict the switching behavior of switches S1 and S3, respectively. It is important to note that in this power direction, the switching losses are caused by the corresponding antiparallel diodes of each switch, which conduct the triangle current.

As can be observed, S3's turn-on procedure causes losses in S1's antiparallel diode as this final device had been conducting the whole current and so had a significant quantity of stored charge. When S1 turns on, the charge in its antiparallel diode is evacuated via S3, resulting in turn-on losses in this final device as well.

According to the waveforms displayed in Figure 9, a modified modulation method may be used, in which S1 cuts off a certain quantity of current. By evacuating the stored charge acquired during its conduction phase through the load, S3's voltage is lowered prior to the application of its gate signal, resulting in ZCS in this final device.

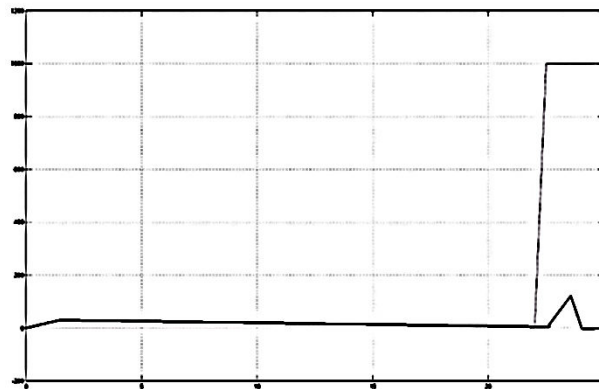


fig:5 current and voltage waveforms in IGBT switches

VII. CONCLUSIONS

The behavior of the internal charge dynamics in HV semiconductors has been seen by analytical and experimental investigations. With the use of this analytical model, which focuses on calculating internal charge behavior for soft-switching applications, switching losses may be estimated without the requirement to do a full switching transient simulation in a circuit simulator. Furthermore, the straightforward analytical model may be employed in a system-wide optimization process in which the switching losses of the converter can be estimated without the need for a circuit simulator, such as the Hefner or HiSIM IGBT models. A detailed description of the conducted tests has also been provided, which allow the model parameters to be extracted. Additionally, while examining the previously suggested ZCS methods for resonant converters. The following were found to be the primary tactics that lower switching losses in MV MF applications:

1) achieving ZVS in the turn-on events; and 2) tailoring the current through the semiconductors to permit a high internal carrier recombination in the device prior to the blocking voltage being reapplied. Both of these methods were used in a TCM DAB. At 120 °C junction temperature, a decrease of up to 40% was attained by attaining ZVS in the turning-on events. A saturable inductor connected in series with the converter's primary inductor shapes the current in the device. In order to achieve high stored charge recombination, this component's current was easily tailored to remain in a low value before the device reaches the blocking state.

REFERENCES

- 1) Bellamkonda Dwiza, Student Member, IEEE [1], "Analysis of Common-Mode Noise and Design of a Reduced-Volume Concentric Choke for Dual Active Bridge dc-dc Converter with Integrated Magnetics" IEEE Trans. Ind. Appl., vol. 27, no. 1, pp. 63–73, Feb.1991.
- 2) Shaoduo Zheng 1,2,3 and Feng Lyu 1,2,3[2], "Compact Medium Voltage DC/DC Converter Using Series-Connected Power Devices" IEEE TRANS:4 June 2020; Accepted: 18 June 2020; Published: 21 June 2020
- 3) Qiang Ren, Fei Xiao, Jilong Liu, Peng Chen, and Zhichao Zhu [3], "Efficiency Improvement and High-performance Control of Dual-active-bridge DC-DC Converter with Triple-phase-shift Modulation" DOI: 10.17775/CSEEJPES.2021.02880, CSEE Journal of Power and Energy Systems.
- 4) Tole Sutikno, Rizky Ajie Aprilianto, and Hendril Satrian Purnama [4], "Application of non-isolated bidirectional DC-DC converters for renewable and sustainable energy systems" Clean Energy, 2023, Vol. 7, No. 2, 293–311 Advance access publication 25 March 2023.
- 5) Xiaotian Zhang, Member, IEEE and Timothy C. Green, Senior Member, IEEE [5], "The Modular Multilevel Converter for High Step-Up Ratio DC-DC Conversion" 10.1109/TIE.2015.2393846, IEEE Transactions on Industrial Electronics IEEE TRANSACTIONS ON INDUSTRIAL ELECTRONICS.
- 6) Venkata Govardhan Rao K, Kumar MK, Goud BS, Bajaj M, Abou Houran M and Kamel S (2022) [6], "Design of a bidirectional DC/DC converter for a hybrid electric drive system with dual-battery storing energy" Front. Energy Res. 10:972089. doi: 10.3389/fenrg.2022.972089
- 7) Atallah, H.; Iqbal, T.; Khalil, I.U.; Ali, U.; Blazek, V.; Prokop, L.; Ullah, N. [7], "Analysis of the Dual Active Bridge-Based DC-DC Converter Topologies, High-Frequency Transformer, and Control Techniques". Energies 2022, 15, 8944. <https://doi.org/10.3390/en15238944>
- 8) Lan Ma, Hongbing Xu, Alex Q. Huang, Jianxiao Zou and Kai Li [8], "IGBT Dynamic Loss Reduction through Device Level Soft Switching" Energies 2018, 11, 1182; doi:10.3390/en11051182
- 9) K.V. Govardhan Rao, Dr.K. Shashidhar Reddy, T. Yedukondalu, [9], "Renewable Energy Source Fed High Step Up Dc-Dc Converter for Distribution Grid Applications" e-ISSN: 2348-6848 p-ISSN:2348-795X Volume 04 Issue 14 November 2017
- 10) Klayani Thalanki, K V Govardhan Rao [10], "AN IMPROVED BIDIRECTIONAL DC/DC CONVERTER WITH SPLIT BATTERY CONFIGURATION FOR ELECTRIC VEHICLE BATTERY CHARGING/DISCHARGING" Aut Aut Research Journal ISSN NO: 0005-0601
- 11) Muthubalaji, S., Kareem, M. A., Karuppiah, N., & Sugirtha, M. G. (2017, December). An enhanced analysis of two diode model PV module under various weather conditions. In 2017 IEEE International Conference on circuits and systems (ICCS) (pp. 162-167). IEEE.



INTERNATIONAL
STANDARD
SERIAL
NUMBER
INDIA



INTERNATIONAL JOURNAL OF INNOVATIVE RESEARCH

IN SCIENCE | ENGINEERING | TECHNOLOGY

 9940 572 462  6381 907 438  ijirset@gmail.com



www.ijirset.com

Scan to save the contact details